Effects of mortar compressive strength on out of plane response of unreinforced masonry walls

Atabak Pourmohammad Sorkhab (Main Author and Corresponding Author)
Istanbul Technical University
34469, Maslak-Istanbul (Turkey)
Sorkhab16@itu.edu.tr
https://orcid.org/0000-0001-9210-6109

Mesut Küçük
Istanbul Technical University
34469, Maslak-Istanbul (Turkey)
kucukmes18@itu.edu.tr
https://orcid.org/0000-0002-8137-9096

Ali Sari
Istanbul Technical University
34469, Maslak-Istanbul (Turkey)
asari@itu.edu.tr
https://orcid.org/0000-0002-6888-1276

Manuscript Code: 28291
Date of Acceptance/Reception: 31.05.2021/13.06.2020
DOI: 10.7764/RDLC.20.2.371

Abstract
In this study, the out-of-plane response of infill walls that are widely used in Turkey and the surrounding regions were experimentally investigated. Several out-of-plane wall tests were performed in the laboratory, with the walls specimens produced with lateral hollow clay bricks (LHCB) and different mortar qualities. The walls were tested in their out-of-plane (OOP) direction under static load conditions and evaluated based on the load-bearing and energy dissipation capacities, crack propagations, mortar strengths, and initial stiffnesses. These walls are experimentally investigated to understand the effects of the mortar strength on the infill wall structural behaviors and to assess the effectiveness of the out-of-plane strength formulations. It was found that when the mortar strength is low, the first major crack occurs at the mortar, however, because of the arch mechanism efficiency in this situation the OOP load-carrying and energy dissipation capacities of unreinforced walls can be significantly increased. When the first major crack in the wall occurs in the brick itself, the arc mechanism is provided with delicate sections in the brick, which leads to strength decreasing in the walls. In this case, excessive deviations occur in the out-of-plane strength formulations estimates. This study shows that the arc mechanism, the damage start region and progress can change significantly unreinforced masonry (URM) infill walls behaviors.

Keywords: lateral hollow clay bricks, infill walls, out-of-plane loadings, mortar compressive strength, experimental OOP test.

Introduction

Infill walls are used in framed structures, specially constructed with reinforced concrete. In these structures, as shown in Figure 1, the exterior faces of buildings are mostly occupied by these walls, which makes the building vulnerable to the exterior horizontal loads. Mainly OOP load cases can cause the infill wall damages, and this load cases occurred by human-made hazards such as acts of terrorism (Figure 2), under extreme natural events, such as strong earthquakes (Figure 1). Under these conditions, the infill walls need strengthening if their structural performances is not satisfactory.

Figure 1. Out-of-plane failures of infill walls. (A) 1999 Kocaeli earthquake. (B) 2011 Van earthquake (Onat, Correia, Lourenço, & Koçak, 2018).

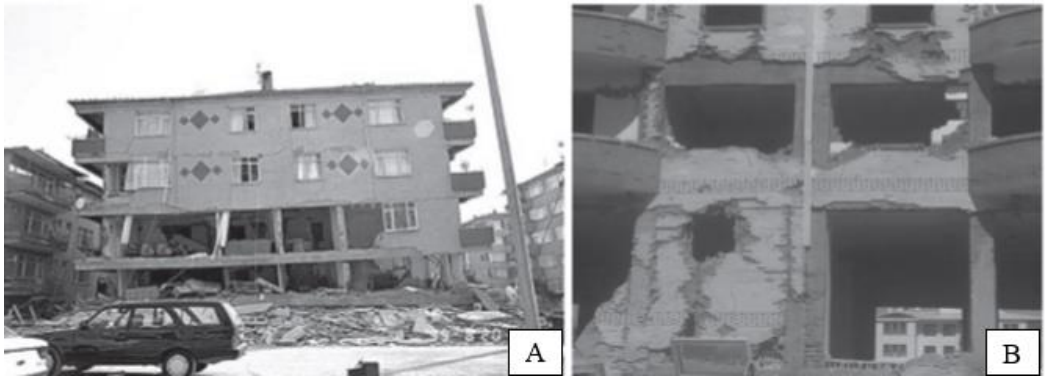

Figure 2. Collapsed infill walls of a State building in Turkey due to an intentional explosion (Yenisafak, 2016).

A vast range of studies was performed in the literature because of the material and usage varieties of the infill or masonry walls in real life. These studies include investigation influence of different parameters(height-to-thickness ratio adherence, axial load, strengthening etc.) on the behavior of infill walls (Angel R, 1994; da Porto, Guidi, Verlato, & Modena, 2015; Demirel, yakut, & binici, 2018; Di Domenico, Ricci, & Verderame, 2019; André Furtado, Rodrigues, Arêde, & Varum, 2018; Sayın B., 2005; Silva, 2020; Valluzzi, da Porto, Garbin, & Panizza, 2014).

These studies were performed in-plane (IP), OOP, or some combination of these load directions. The IP and combination of IP and OOP direction studies were mostly preferred to understand the behavior of walls under seismic actions that can cause failure and collapse of the infill walls. The main goals of these studies have been to prevent loss of life and economic losses. Some of the previous studies also included improvement of the frame's structural performance by strengthening the infill walls with various methods or using other infill materials (Arslan, Durmuş, & Hüsem, 2019; Binici et al., 2019; Ricci, Di Domenico, & Verderame, 2018). Pure OOP investigations for infill walls are mostly concerned about two situations: the first is that pieces of infill wall fall on people and valuable things during an earthquake. Second, walls are directly exposed to pressure (in a dynamic or shock manner) by air or flying objects, maybe during an explosion. In the previous studies, the researchers mostly investigated parameters affecting the infill walls' OOP behavior, such as slenderness, boundary conditions, strengthening technics, loading cases, etc.

Under OOP loading one-way or two-way arching can occur in the infill walls and It can be observed that the OOP strength provided by two-way arching action is higher than by one-way arching and that walls with low slenderness have higher stiffness and strength than the high slenderness (Di Domenico et al., 2019). In the literature, it is stated that the out-of-plane behavior of the infill walls built within the RC frame is largely affected by the adherence between the frame and the infill wall rather than the high ductility or low ductility of the frame (André Furtado et al., 2018). Several experimental studies were performed to understand the effects of different boundary conditions on OOP stiffness, strength, and displacement capacity of unreinforced infill walls and assessing the contribution of vertical and horizontal arching action to their OOP response (Di Domenico, Ricci, & Verderame, 2020; Dizhur, Ingham, Walsh, Giongo, & Derakhshan, 2018). In these studies, it was concluded that OOP strength was the highest for the test specimen restrained along all edges, lower for the one restrained along three sides, and the weakest for the one restrained along two edges. Furtado et al. (2020) investigated the out-of-plane behavior of the infill wall, the lower surface of which was supported with reinforced concrete at a ratio of 2/3. In this case, it was evaluated that the out-of-plane stability and strength of the wall decreased, but the arch mechanism occurred in the wall provided a sufficient strength capacity to prevent the wall from collapsing. (A. Furtado, Arêde, Varum, & Rodrigues, 2020).

In this paper, the effect of mortar compressive strengths on the out-of-plane response of unreinforced masonry walls was studied. Productions of these walls differ from some regions to another or even in the same area and this case is borning new problems to understanding walls behaviors. There was not much attention to mortar quality effects on infill wall behaviors in the literature. Thus, in this study, several infill walls are constructed with materials produced in Turkey and neighboring countries. The walls were bound to the confining reinforced concrete beams along two edges. These walls are experimentally investigated to understand the effects of the mortar strength on the infill wall structural behaviors. Experimental results of this study were compared with another study that used almost the same slenderness ratio and two edges bounded specimens. Further, the test results were compared with some mathematical models produced to two edges bounded infill walls, and the suggestion was given to update these models according to the wall damage shape differences caused by mortar strength.

Studies on two edges bounded URM infill walls

There are some experimental and mathematical models researches in the literature for infill walls bounded on two edges. At the same time, these studies investigated the effects of boundary conditions on infill walls pure out-of-plane behavior and load-carrying capacities. Di Domenico et al. (2019) have performed some experimental test on two edges bounded walls having two different slenderness ratios. In the experiments, a four-point loaded in the direction of out-of-plane are applied to specimens. In the study, it was found that higher slenderness ratio results in lower out of plane strength and energy dissipation capacity of the wall. Also, the study shows that OOP strength was the highest for the test specimen restrained along all edges, lower for the one restrained along three edges, and the weakest for the one restrained along two edges.

Out-of-plane strength models proposed by Angel et al. (1994) and Eurocode 6 (2004) can calculate strength of unit-width masonry stripe bounded by two (upper and bound) edges (Angel R, 1994; Eurocode, 2004). These models have been obtained by assuming uniformly distributed out-of-plane load on the wall. Eqs. 1 and 2 are for Angel et al. (1994) and Eurocode 6 (2004) models, respectively. These models formulations were not directly taken from their source but the original form of them checked and be supplied as stated from Di Domenico et al. (2019) study since in the study, formulations have been explained handy. In these equations,f_{mv} is the strength of masonry in compression in the vertical direction, both expressed in N/mm^2: h is the infill height expressed in *mm*, w is the infill width expressed in *mm*, t is the infill thickness expressed in *mm*. F_{max} is the out-of-plane strength expressed in *N*.

$$F_{max} = \frac{2f_{mv}}{(h/t)}\lambda R_1 R_2 wh \qquad (1)$$

$$F_{max} = f_{mv}\left(\frac{t}{h}\right)^2 wh \qquad (2)$$

$$\lambda = 0.154e^{-0.0985(h/t)} \qquad (3)$$

In Eq. 1, λ is a slenderness factor, R_1 is a factor accounting for the out-of-plane resistance degradation due to in-plane damage, R_2 is a factor accounting for the flexural deformability of the reinforced concrete frame elements. For the current study, R1 is selected 1.0 since there is no in-plane resistance degradation and R2 is selected 1.0 to make a suitable comparison with Eurocode 6 (2004)'s strength model which assumes that the confining frame elements are stiff. The λ factor can be calculated by means of the expression proposed by Flanagan and Bennett (1999) and reported in Eq. 3 [17]. In Eq. 3, h is the infill height, t is the infill thickness, both expressed in consistent unit of length. Eq. 2 has a conservative simplification applied by Eurocode 6 (2004). The original formulation is reported in Eq. 4.

$$F_{max} = 1.08f_{mv}\left(\frac{t}{h}\right)^2 wh \qquad (4)$$

Experimental study

The experimental phase of the study is described in this section. Material properties are detailed and then test setup and the instrumentation system are shown. Four specimens have been designed, constructed, and tested. All specimens have been tested under pure out-of-plane load.

Material properties

For all bricks used in wall test samples, it was ordered to be in the dimension of 124 mm x 190 mm x 190 mm , and it was taken from one production. Mechanical properties of bricks were determined with compression tests (Figure 3). Compressive strengths and elasticity modules of samples are given in Table 1. Mortars prepared with three different ratios were used in the construction of the walls. These mortar ratios were determined as 3:0.5:1.0 (A), 3:1.0:1.5 (B) and 3:1.5:1.5 (C) (send: water: cement). In order to determine the mortar compressive strength and elasticity modules, 3 pieces of 10 cm x 20 cm cylinder samples were tested for each group of mixture ratios on the same day as the wall experiments (Figure 4). The samples were tested according to ASTM C469 / C469M code and compressive strengths and elasticity modules of samples are given in Table 2.

Figure 3. LHCB's compression test and strain measurement. (Self-Elaboration).

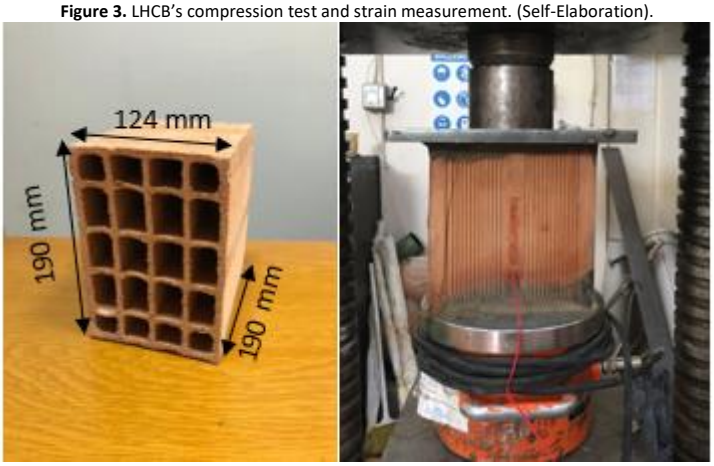

Figure 4. Mortar compression test and strain measurement. (Self-Elaboration).

Table 1. Mechanical properties of LHCB`s. (Self-Elaboration).

Mechanical property	Mean value
Compressive Strength (parallel to holes), N/mm^2 Cov (%)	6.6 (3.03)
Elasticity Modules (parallel to holes), N/mm^2 Cov (%)	4480 (27.29)
Compressive Strength (perpendicular to holes), N/mm^2 Cov (%)	1.79 (11.73)

Table 2. Mechanical properties of mortars.

Mechanical property	A (Mean)	B (Mean)	C (Mean)
Compressive Strength, N/mm^2 Cov (%)	18.30 (9.04)	12.99 (7.77)	8.36 (2.87)
Elasticity Modules, N/mm^2 Cov (%)	15079 (6.32)	16090 (23.34)	10085 (7.516)
Mixture Volume ratios (send: water: cement)	3:0.5:1.0	3:1.0:1.5	3:1.5:1.5

Description of test setup

Four test specimens were investigated within the study. Wall samples were named W1, W2, W3, and W4 that were constructed with A, B, C, and again A mortars, respectively. The dimension of the walls was selected as 161 cm × 135 cm × 12.4 cm. Two 15 cm x 15 cm x 135 cm reinforced concrete beams are attached to the top and bottom of the walls, which simulates infill walls that are bounded on two edges. Dimension details of the walls are shown in Figure 5. Each specimen was loaded in the middle of their height laterally by an Actuator that has a 25-ton capacity and fixed on a strong wall. 10 cm x 10 cm x 135 cm steel box is used to spread the load and rubber material is used to prevent local damage. The actuator-sample reaction system is shown in the Figure. The OOP load was applied in displacement control with OOP displacements monotonically increasing at 0.02 mm/s velocity. Linear Variable Displacement Transducer (LVDTs) were placed at 3 height point of the walls to measure the displacements (Figure 5).

Figure 5. Wall layout and test instrumentation setup. (Self-Elaboration).

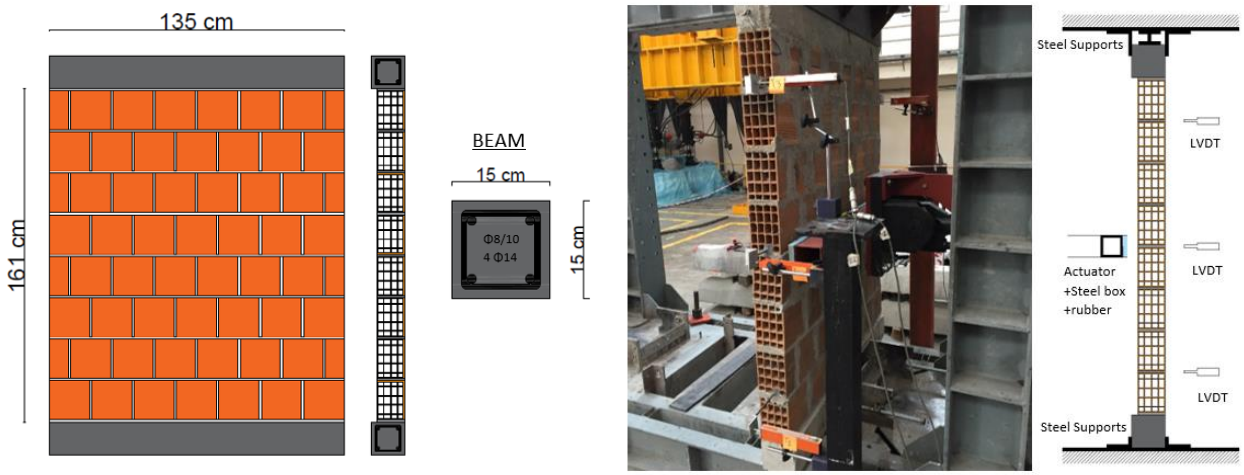

Test results

The walls were placed to the test setup after mortars gained their strengths. Structural behaviors of the specimens were investigated based on the load-carrying and energy dissipation capacities, crack propagations, mortar strengths, and initial stiffness. Lateral load-displacement curves of the walls are presented in Figure 6. When the walls carrying capacities are compared, it is seen that W3 had the most carrying capacity. Crack propagations of each specimen can be seen in Figure 7. In the W1 and W4, the first major crack was observed in the horizontally arranged bricks in the middle of the walls. In W2 the first major cracks were observed mostly in bricks and partly in brick mortar interfaces whereas, in the W3 sample, the first crack occurred in the middle of the wall along with the horizontal mortar and mortar brick interface due to the weak mechanical properties of the mortar. In all samples, one-way arc-mechanism was observed after the first crack. In Table 3, load-carrying capacities, first crack loads, and initial stiffness of the walls are listed. It was seen that W3 had more energy dissipation capacity and maximum load-bearing capacity than other specimens (Figure 8).

Figure 6. Load-displacement curves of each URM walls. (Self-Elaboration).

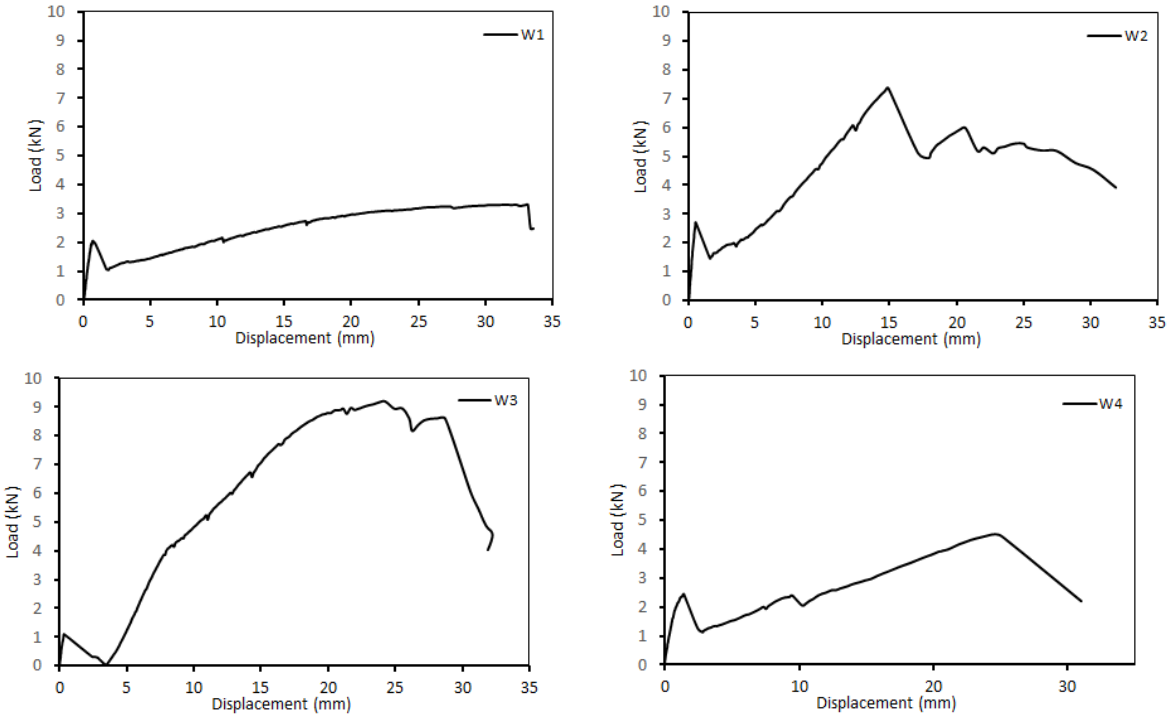

Figure 7. Crack propagation of each specimen at the end of the test. (Self-Elaboration).

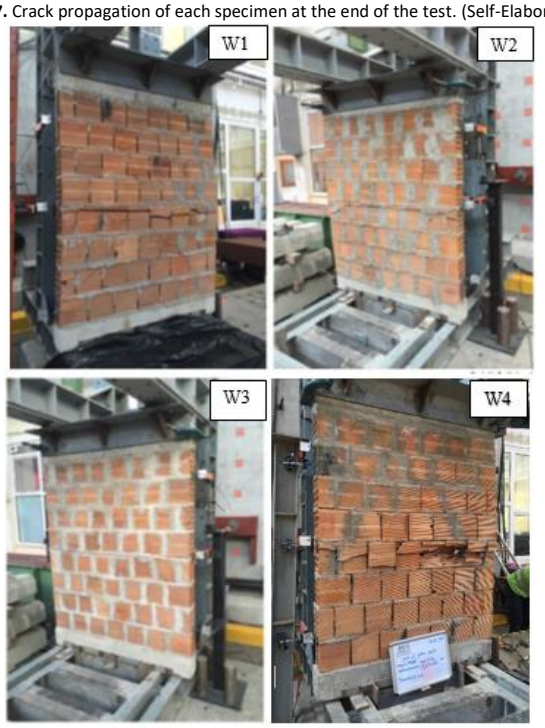

Figure 8. Energy dissipation and maximum load capacities of the walls and mortar compressive strengths. (Self-Elaboration).

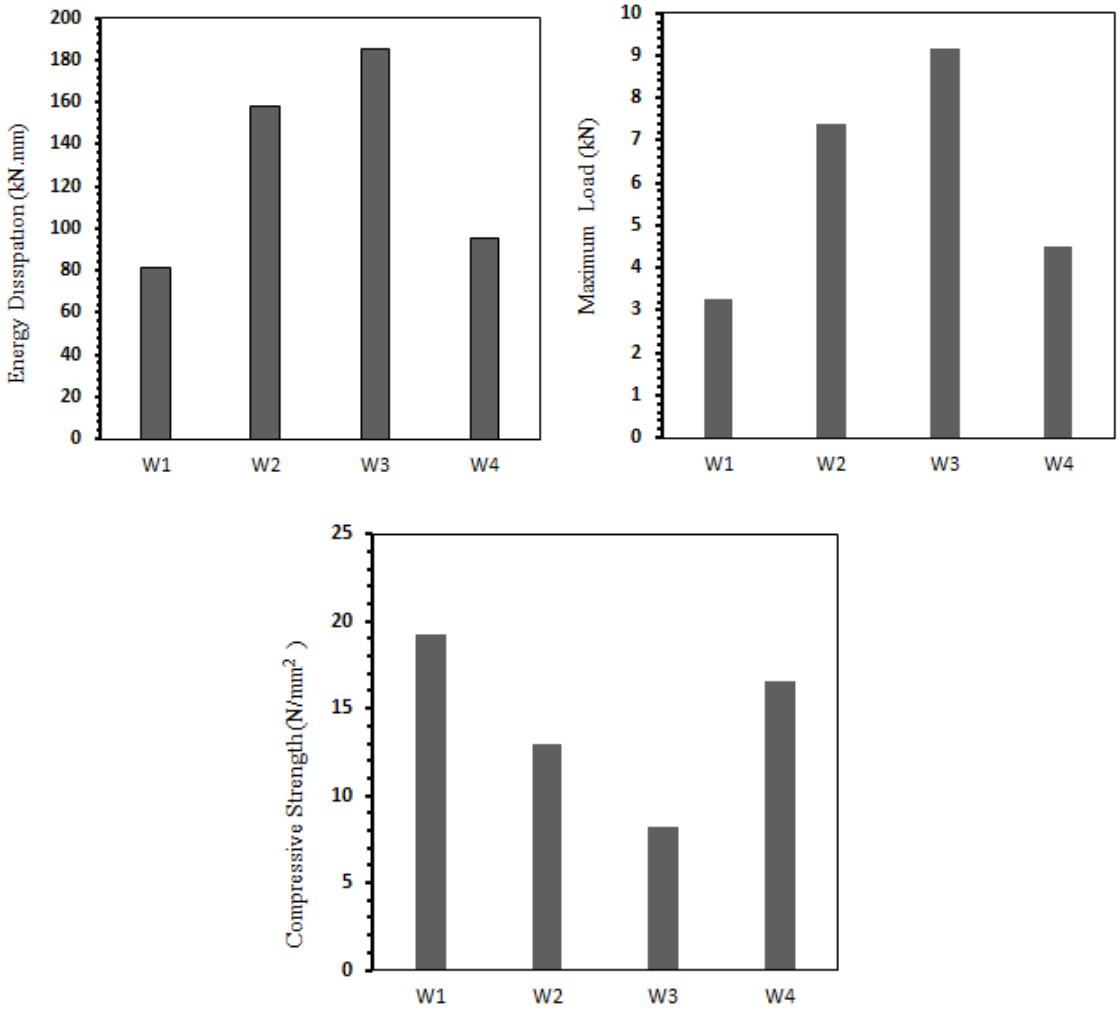

Table 3. Experimental results of walls. (Self-Elaboration).

Specimen	Maximum Load (kN) fm	First crack Load (kN) fcr	Lateral Initial Stiffness kN/mm Ki	Energy Dissipation Capacity (kN.mm) Ed	Used Mortar Strength (MPa) fm
W1	3.28	2.03	3.68	81.23	18.30 (A)
W2	7.37	2.7	5.93	158.41	12.99 (B)
W3	9.17	1.08	3.42	185	8.36 (C)
W4	4.5	2.44	2.51	95	18.30 (A)

It is seen that from this result when mortar strength is decreased the energy dissipation and maximum load-bearing capacities of walls are increasing. Actually, this situation caused by not directly mortar strength but by indirectly with mortar affecting crack propagation of specimens. The occurrence of the first major crack only throughout the mortar or mortar-brick interface causes the low first crack load. Because of using the same type of brick when crack occurred throughout the brick, it was observed that the first major crack load of W1, W2 and W4 are very close and higher than W3. In W1, W2, and W4, the first major crack load of the specimens increased respectively by 88%, 150%, and 125% according to W3, a specimen having a first major crack along horizontal mortar-brick interface. However, W3 had higher maximum load-bearing than other specimens, because the arc mechanism worked effectively in the specimen.

According to the test results, the behavior of the walls is summarized and schematized as in Figure 9. In figure 9, two main factors affecting wall behaviors are discussed. These are where the first major crack occurred and the wall boundary conditions. The reason that the load suddenly decreases after the first crack is that there is a certain degree of freedom of rotation in the wall supports. At the end of this freedom of rotation, the wall starts to reload and goes up to the maximum load. When looking at the test results, differences were found in the behavior of the walls to reach maximum load levels. These behavioral differences were evaluated as in Figure 9. Here, when the first crack in the wall occurs in the brick itself, the arc mechanism is provided with delicate sections in the brick, which leads to almost 50% reduction in the load-bearing and energy dissipation capacities of the walls.

Figure 9. Crack propagation and limited support rotation factors affecting the wall behaviors. (Self-Elaboration).

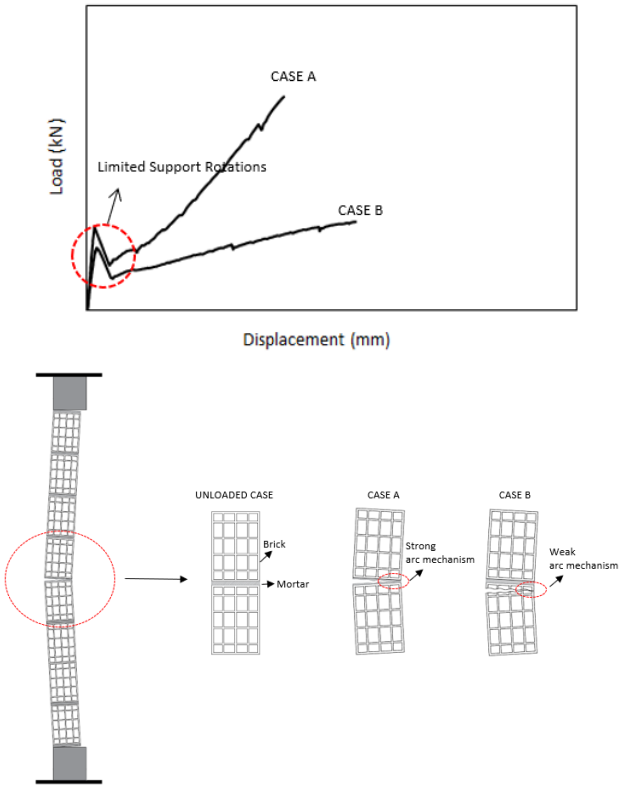

In this section, the pure OOP strength of the specimens are discussed. Abovementioned the models calculating the two bounded infill wall OOP strength were used and their results compared with the experimental test results of current study. Formulations are multiplied by a factor equal to 0.50 to obtain comparable results under a three-point load with loading points placed at half of the infill length in the direction of out-of-plane as in the current study since the literature formulations are improved by uniform load assumption. This factor is calculated as in the study of Di Domenico et al (2019) that is obtaining the factor, s_{fd} by calculating the ratio between the external work done by a uniformly distributed load, $L_{E,ud}$ reported in Eq 5, and that done by a four-point load, $L_{E,4f}$ reported in Eq 6. These equations are obtained by considering the stripe deformed shape/mechanism reported in Figure 10c-d. External work done by a three-point load $L_{E,f}$ as in the current study reported in Eq. 7, while the loading condition is defined as Figure 10e. The value obtained for the conversion factor, s_{fe} is reported in Eq 9. The converted out-of-plane strengths obtained by formulations for all specimens are shown in Table 4.

Figure 10. Deformed shape of an infill stripe under OOP load after first cracking Di Domenico et al (2019).

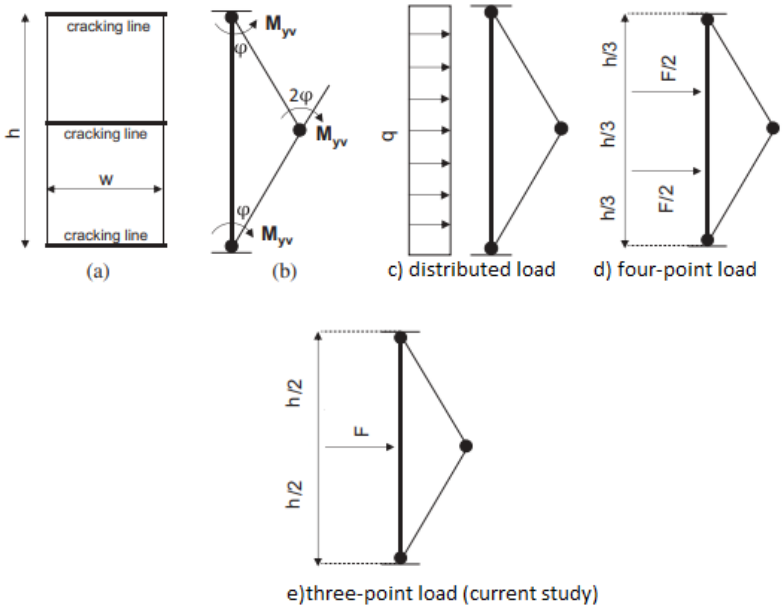

$$L_{E,ud} = qwh\frac{h}{4}\phi = F\frac{h}{4}\phi \quad (5)$$

$$L_{E,4F} = 4\frac{F}{4}\frac{h}{3}\phi = F\frac{h}{3}\phi \quad (6)$$

$$L_{E,F} = F\ \frac{h}{2}\phi = F\frac{h}{2}\phi \quad (7)$$

$$s_{Fd} = \frac{L_{E,4F}}{L_{E,ud}} = \frac{3}{4} = 0.75 \quad (8)\ \text{[Di Domenico et al. (2019)]}$$

$$s_{Fe} = \frac{L_{E,F}}{L_{E,F}} = \frac{2}{4} = 0.5 \quad (9)\ \text{[current study]}$$

Also, experimental results in Di Domenico et al. (2019)'s study are compared with current study in this section. For an appropriate comparison, Di Domenico's four-point load test results are converted to three-point load test results. For this reason, a new load condition factor, l_{cf} is calculated by dividing the three-point load factor, s_{fe} by the four-point load factor, s_{fd}. At the same time, because of the geometric differences between Di Domenico et al (2019)'s and the current study, the geometric part of Eq.4 is used to obtain the geometric conversion factor, g_{cf}. Experimental out-of-plane strength of specimens in Di Domenico et al (2019)'s study multiplied by $(l_c)x(g_c)=0.528$ so that it can be comparable with current study. All these informations are reported in Table 5.

As seen in Table 4, Eurocode 6 (2004) gives very close results with ratios equal to 0.73 for W3 specimen. On the other hand, Angel et al. (1994)'s model also is overestimates the strength of all specimens. It should be noted that both models are overestimating but provide more close results of the out-of-plane strength of W3 since this specimen crack

propagation almost fits with selected models hypothesis. However, as mentioned before in Figure 9, when the first major crack in the wall occurs in the brick itself, the arc mechanism is provided with delicate sections in the brick, which leads to strength decreasing in the other walls. In this case, excessive deviations occur in the models estimates.

As seen In Table 5, W3 has good agreement with Di Domenico et al. (2019)'s test results. Because in Di Domenico et al. (2019)'s the study, the specimen is constructed with low strength mortar that leads to crack propagation in the mortar-brick interface and then to a strong arch mechanism as observed in W3.

Table 3. Comparison of the experimental and predicted out-of plane strength of specimens. (Self-Elaboration).

Specimen	Current Study Maximum Load (kN)	Eurocode 6 (2004)		Angel et al. (1994)		Current Study Mortars Strengths (MPa)
		Pred. (kN)	Exp/ Pred	Pred (kN)	Exp/ Pred	
W1	3.28	12.46	0.26	12.84	0.25	18.30
W2	7.37	12.46	0.59	12.84	0.57	12.99
W3	9.17	12.46	0.73	12.84	0.71	8.36
W4	4.5	12.46	0.36	12.84	0.35	18.30

Table 4. Comparison of the experimental out-of-plane strength of specimens. (Self-Elaboration).

Specimen	Current Study Strength Exp. (kN)	Di Domenico et al. (2019) Exp. Original (kN)	Di Domenico et al. (2019) Converted (kN)	Di Domenico et al. (2019) Mortars Strengths (MPa)	Current Study Mortars Strengths (MPa)	Proportion of Mortars Strengths	Proportion of Wall Strengths
W1	3.28	24.0	12.672	8.29	18.30	0.45	0.26
W2	7.37	24.0	12.672	8.29	12.99	0.63	0.58
W3	9.17	24.0	12.672	8.29	8.36	0.99	0.72
W4	4.5	24.0	12.672	8.29	18.30	0,45	0.35

Conclusions

Within the study, the out-of-plane response of URM infill walls having different mortar strengths were investigated. The main aim of the study is to assess the effect of different mortar strength on the out-of-plane response of infills wall and prediction efficiency of literature and code provisions to the out-of-plane strength due to changes in mortar quality.

The maximum load-carrying capacities of specimens were not increased by increasing the mortar strength. Inversely, the W3 wall had the most load-carrying and energy dissipation although it had the weakest mortar. This case shows that the wall failure mechanism is very important in terms of maximum load-carrying capacity. Because constructing the specimen with low strength mortar leads to crack propagation in the mortar-brick interface or in the mortar and then to a strong arch mechanism as observed in the current study tests.

Eurocode 6 (2004)'s and Angel et al. (1994)'s formulations for the specimens bounded along two edges in which only one-way vertical arching occurs showed best predicting performance for specimen have mortar-brick interface crack propagation. But specimens constructed with high strength mortars had a first major crack at the brick, which leads to a weak arch mechanism and then to overestimate results for literature formulations. The occurrence of limited support rotations in all wall samples tested in this study is also considered to have an effect on the deviations in the results.

In this study, it is assumed that there is a directly proportional relationship between the mortar compressive strength and the brick-mortar bond strength and that mortar compressive strength indirectly has an impact on the wall crack propagation that affects the wall OOP strength. It is suggested that the correlation between the mortar compressive and brick-mortar bond strength should be determined by performing some experiments.The results presented in this paper should be extended in future works with the assessment of three and four edges bounded URM infill walls. Also, with more tests, strength predicting formulations can be modified for the effect of mortar strength on crack propagation shape.

Acknowledgements

This study was supported by the Scientific Research Projects Commission of Istanbul Technical University under grant number MGA-2017-40726 and MDK-2019-42161.

References

Angel R, A. D., Shapiro D, Uzarski J, Webster M. (1994). Behaviour of reinforced concrete frames with masonry infills.

Arslan, M. E., Durmuş, A., & Hüsem, M. (2019). Cyclic behavior of GFRP strengthened infilled RC frames with low and normal strength concrete. Science & Engineering of Composite Materials, *26*(1), 30. doi:https://doi.org/10.1515/secm-2017-0060

Binici, B., Canbay, E., Aldemir, A., Demirel, I. O., Uzgan, U., Eryurtlu, Z., . . . Yakut, A. (2019). Seismic behavior and improvement of autoclaved aerated concrete infill walls. Engineering Structures, *193*, 68-81. doi: https://doi.org/10.1016/j.engstruct.2019.05.032

Bombing news in Turkey. (2016). Yenisafak, pp. https://www.yenisafak.com/gundem/midyatta-emniyet-mudurlugune-bombali-aracla-saldiri-2477659.

Da Porto, F., Guidi, G., Verlato, N., & Modena, C. (2015). Effectiveness of plasters and textile reinforced mortars for strengthening clay masonry infill walls subjected to combined in-plane/out-of-plane actions/Wirksamkeit von Putz und textilbewehrtem Mörtel bei der Verstärkung von Ausfachungswänden aus Ziegelmauerwerk, die kombinierter Scheiben- und Plattenbeanspruchung ausgesetzt sind. Mauerwerk, *19*(5), 334-354. doi:https://doi.org/10.1002/dama.201500673

Demirel, i. o., yakut, a., & binici, b. (2018). Dolgu Duvarların Düzlem Dışı Yönde Hava Yastığı İle Deneyi. Anadolu Üniversitesi Bilim Ve Teknoloji Dergisi - B Teorik Bilimler, 6(2), 133-140. doi:https://doi.org/10.20290/aubtdb.489940

Di Domenico, M., Ricci, P., & Verderame, G. M. (2019). Experimental assessment of the out-of-plane strength of URM infill walls with different slenderness and boundary conditions. Bulletin of Earthquake Engineering, *17*(7), 3959-3993. doi: https://doi.org/10.1007/s10518-019-00604-5

Di Domenico, M., Ricci, P., & Verderame, G. M. (2020). Experimental Assessment of the Influence of Boundary Conditions on the Out-of-Plane Response of Unreinforced Masonry Infill Walls. Journal of Earthquake Engineering, *24*(6), 881-919. doi: https://doi.org/10.1080/13632469.2018.1453411

Dizhur, D., Ingham, J., Walsh, K., Giongo, I., & Derakhshan, H. (2018). Out-of-plane Proof Testing of Masonry Infill Walls. Structures, *15*, 244-258. doi:https://doi.org/10.1016/j.istruc.2018.07.003

Eurocode. (2004). Design of masonry structures. Part 1-1: General Rules for Reinforced and Unreinforced Masonry Structures. In.

Flanagan, R. D., & Bennett, R. M. (1999). Arching of Masonry Infilled Frames: Comparison of Analytical Methods. Practice Periodical on Structural Design & Construction, *4*(3), 105. doi:https://doi.org/10.1061/(asce)1084-0680(1999)4:3(105)

Furtado, A., Arêde, A., Varum, H., & Rodrigues, H. (2020). Effect of the Panel Width Support and Columns Axial Load on the Infill Masonry Walls Out-Of-Plane Behavior. Journal of Earthquake Engineering, *24*(4), 653-681. doi: https://doi.org/10.1080/13632469.2018.1453400

Furtado, A., Rodrigues, H., Arêde, A., & Varum, H. (2018). Out-of-plane behavior of masonry infilled RC frames based on the experimental tests available: A systematic review. Construction and Building Materials, *168*, 831-848. doi:https://doi.org/10.1016/j.conbuildmat.2018.02.129

Onat, O., Correia, A. A., Lourenço, P. B., & Koçak, A. (2018). Assessment of the combined in-plane and out-of-plane behavior of brick infill walls within reinforced concrete frames under seismic loading. Earthquake Engineering and Structural Dynamics, *47*(14), 2821-2839. doi:https://doi.org/10.1002/eqe.3111

Ricci, P., Di Domenico, M., & Verderame, G. M. (2018). Experimental assessment of the in-plane/out-of-plane interaction in unreinforced masonry infill walls. Engineering Structures, *173*, 960-978. doi:https://doi.org/10.1016/j.engstruct.2018.07.033

Sayın B., K. S. A. (2005). Deprem etkisi altındaki betonarme yapılarda dolgu duvarların modellenme teknikleri Paper presented at the Deprem Sempozyumu, Kocaeli.

Silva, Y. F., Lange, D. A., & Delvasto, S. (2020). Effects of the incorporation of residue of masonry on the properties of cementitious mortars. Revista de la Construcción. Journal of Construction, *19*(3), 407-421. doi:https://doi.org/10.7764/rdlc.19.3.407-421

Standard Test Method for Static Modulus of Elasticity and Poisson's Ratio of Concrete in Compression. (2014). In ASTM C469 / C469M-14. West Conshohocken, PA: ASTM International.

Valluzzi, M. R., da Porto, F., Garbin, E., & Panizza, M. (2014). Out-of-plane behaviour of infill masonry panels strengthened with composite materials. Materials and Structures/Materiaux et Constructions, *47*(12), 2131-2145. doi:https://doi.org/10.1617/s11527-014-0384-6